BRIGHTNESS AND COHERENCE OF SYNCHROTRON RADIATION AND FELs*

Zhirong Huang
SLAC National Accelerator Laboratory, Menlo Park, CA 94025, USA

Abstract

This paper reviews the brightness and coherence properties of radiation from storage rings and free electron lasers (FELs). Starting from the statistical optics and using mutual coherence function of the radiation field, we define the transverse and temporal coherence and modes. Spectral brightness can be represented in radiation phase-space via the Wigner function which is the Fourier transformation of the transverse correlation function. The brightness convolution theorem can be employed to calculate the total source brightness and the degree of transverse coherence of the radiation emitted by an electron beam. Undulator radiation possesses partial transverse coherence until the beam emittances can be reduced below the diffraction limit. For x-ray FELs the radiation has excellent transverse coherence and at least 9 orders of magnitude enhancement in peak brightness. Seeding can further improve temporal coherence of FELs. Future development includes diffraction limited light sources, higher peak and average power x-ray FELs and compact coherent radiation sources based on laser and plasma accelerators.

INTRODUCTION

Radiation emission by electrons in an accelerator was first observed in 1946 in a synchrotron at the General Electrical Research Laboratory in New York. This discovery opened a new era of accelerator-based light sources. These light sources have made tremendous progress over the last 60 years and have evolved rapidly through four different generations. The first three generations are based on synchrotron radiation, with the current third-generation facilities relying on effective insertion devices especially undulators as their work horses. The fourth-generation light source is a game-changer that shifts the radiation generation mechanism from synchrotron radiation to the free electron laser (FEL). The brightness of these sources and their coherence properties have improved many orders of magnitude over the years. This impressive growth of capabilities have fostered scientific advances in physics, chemistry and biology as well as practical applications in industry and medicine.

In the next section, we describe both temporal and transverse (spatial) coherence based on the mutual coherence function of a radiation field. In Section 3, we discuss spectral brightness first qualitatively and then quantitatively with the Wigner function. In Section 4, undulator radiation brightness is presented using the Gaussian approximation. Higher brightness and coherence fraction can be reached with smaller beam emittances until the diffraction limit. The dramatic enhancement in brightness and coherence for FEL sources are highlighted in Section 5. Finally, I conclude with my personal perspectives on future research and development for this very dynamic field.

* Work supported by DOE Contracts No. DE-AC02-76SF00515.

COHERENCE

Coherence is a fundamental property of a radiation source. Most light sources including synchrotron radiation and FELs posses a certain degree of coherence. The quantitative description of partial coherence is through the so-called mutual coherence function. Considering a scalar electric field E (of a particular radiation polarization) that propagates along the longitudinal z direction, the mutual coherence function is [1]

$$\Gamma(\boldsymbol{x}_1, \boldsymbol{x}_2, t_1, t_2) = \langle E(\boldsymbol{x}_1, t_1) E^*(\boldsymbol{x}_2, t_2) \rangle \,, \qquad (1)$$

where $\boldsymbol{x} = (x, y)$ represents the transverse coordinates, t is the arrival time of the signal at a particular z location, * means complex conjugate, and brackets $\langle\rangle$ indicate the ensemble average over many radiation pulses. Here z is considered as the independent variable and is suppressed in the expressions as much as possible. The complex degree of coherence is defined as the normalized mutual coherence function as

$$\gamma(\boldsymbol{x}_1, \boldsymbol{x}_2, t_1, t_2) = \frac{\Gamma(\boldsymbol{x}_1, \boldsymbol{x}_2, t_1, t_2)}{\sqrt{I(\boldsymbol{x}_1, t_1) I(\boldsymbol{x}_2, t_2)}} \,, \qquad (2)$$

where $I(\boldsymbol{x}, t) = \Gamma(\boldsymbol{x}, \boldsymbol{x}, t, t)$ is the radiation intensity. Since the typical x-ray pulse duration generated from the electron bunch is much longer than the coherence time (to be defined next) of undulator radiation and FELs, then we can approximate

$$\gamma(\boldsymbol{x}_1, \boldsymbol{x}_2, t_1, t_2) = \gamma(\boldsymbol{x}_1, \boldsymbol{x}_2, t_1 - t_2) \,. \qquad (3)$$

Two classes of coherence are separately discussed. $\gamma(\boldsymbol{x}_1, \boldsymbol{x}_2, 0)$ describes the transverse coherence, while $\gamma(0, 0, \tau)$ characterizes the temporal coherence.

Temporal Coherence

Temporal coherence specifies the extent to which the radiation maintains a definite phase relationship at two different times. Temporal coherence is characterized by the coherence time, which can be experimentally determined by measuring the path length difference over which fringes

Invited to The 4th International Particle Accelerator Conference
Shanghai, China, May 12-17, 2013

Work supported in part by US Department of Energy under contract DE-AC02-76SF00515.

can be observed in a Michelson interferometer. The coherence time τ_c is related to the complex degree of coherence:

$$\tau_c = \int_{-\infty}^{\infty} d\tau |\gamma(\tau)|^2 \,. \tag{4}$$

The Wiener-Khinchin theorem states that the temporal coherence function and the radiation spectrum forms a Fourier pair:

$$\gamma(\tau) = \frac{\int_{-\infty}^{\infty} d\omega |E(\omega)|^2 e^{-i\omega\tau}}{\int_{-\infty}^{\infty} d\omega |E(\omega)|^2} \,. \tag{5}$$

Here $E(\omega)$ is the Fourier transformation of $E(t)$. For a Gaussian radiation spectrum with the rms width σ_ω, Eqs. (5) and (4) lead to

$$\tau_c = \frac{\sqrt{\pi}}{\sigma_\omega} \,. \tag{6}$$

Hence a narrower bandwidth radiation results in a greater temporal coherence. The number of temporal modes for a flattop pulse of duration T is T/τ_c.

Transverse Coherence

Transverse coherence or spatial coherence describes the degree to which the phase of the wave is correlated at two distinct points in the transverse plane. Transverse coherence can be measured via the interference pattern in Young's double slit experiment. The radiation source illuminates two slits located at $\boldsymbol{x}_1$ and $\boldsymbol{x}_2$ at $z = 0$ plane will form an interference pattern at an image screen far from the slits. The total intensity on the screen is given by

$$\begin{aligned} I_{\rm tot} =& \left|\langle E(\boldsymbol{x_1}, t - t_1)\rangle\right|^2 + \left|\langle E(\boldsymbol{x_2}, t - t_2)\rangle\right|^2 \\ &+ 2\mathrm{Re}\left[\langle E(\boldsymbol{x_1}, t - t_1) E^*(\boldsymbol{x_2}, t - t_2)\rangle\right] \\ =& I(\boldsymbol{x}_1) + I(\boldsymbol{x}_2) + 2\sqrt{I(\boldsymbol{x}_1) I(\boldsymbol{x}_2)} \\ &\times \mathrm{Re}\left[|\gamma(\boldsymbol{x}_1, \boldsymbol{x}_2, t_1 - t_2)|\right] , \end{aligned} \tag{7}$$

where t_1 and t_2 are the times taken by signals from each slit to reach the screen at time t, and Eq. (3) is used to simplify the last step. At the center of the screen where $t_1 = t_2$, the fringe visibility is given by the amplitude of the transverse correlation function $\gamma(\boldsymbol{x}_1, \boldsymbol{x}_2, 0)$.

A single parameter can be used to characterize the total degree of transverse coherence (coherent fraction) as:

$$\zeta = \frac{\int\int |\gamma(\boldsymbol{x}_1, \boldsymbol{x}_2, 0)|^2 I(\boldsymbol{x}_1) I(\boldsymbol{x}_2) d\boldsymbol{x}_1 d\boldsymbol{x}_2}{\int I(\boldsymbol{x}_1) d\boldsymbol{x}_1 \int I(\boldsymbol{x}_2) d\boldsymbol{x}_2} . \tag{8}$$

$1/\zeta$ is a measure of radiation transverse mode numbers. A fully transversely coherent source has $\zeta = 1$.

BRIGHTNESS

When there is a beam of electrons with slightly different transverse positions and angles, the radiation characteristics of the total source might be quite different from that of a single electron (see Fig. 1). To describe the radiation phase space properties of many random emitters (electrons), the brightness concept is introduced. Brightness is defined as the photon flux per unit area and per unit solid angle at the source. Brightness is a conserved quantity in perfect optical systems, and thus is a very useful figure of merit in designing synchrotron radiation and FEL facilities. Typical experiments use a monochromator to select a very narrow spectrum, hence it is conventional to define spectral brightness (or brilliance) as

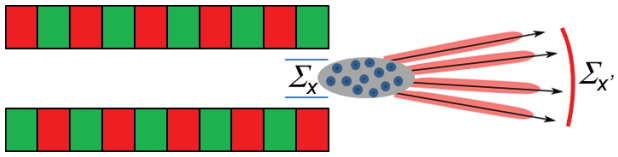

Figure 1: Undulator radiation from an electron beam has effective source size Σ_x and angular divergence $\Sigma_{x'}$ determined by the phase space convolution of single electron radiation and electron beam properties.

$$B \sim \frac{F(\omega)}{\Sigma_x \Sigma_{x'} \Sigma_y \Sigma_{y'} (\Delta\omega/\omega)} \,. \tag{9}$$

Following the phase space methods of Ref. [2], the spectral brightness $B(\boldsymbol{x}, \boldsymbol{\phi}; z)$ is defined on the transverse position-angle phase space $(\boldsymbol{x}, \boldsymbol{\phi})$ via the Wigner transform of the radiation field in the frequency domain:

$$\begin{aligned} B(\boldsymbol{x}, \boldsymbol{\phi}; z) = & \frac{d\omega}{\hbar\omega} \frac{\omega^2 \varepsilon_0}{\pi c T} \int d\boldsymbol{\xi} e^{ik\boldsymbol{\xi}\cdot\boldsymbol{\phi}} \\ & \times \left\langle E\left(\boldsymbol{x} + \tfrac{1}{2}\boldsymbol{\xi}; z\right) E^*\left(\boldsymbol{x} - \tfrac{1}{2}\boldsymbol{\xi}; z\right)\right\rangle . \end{aligned} \tag{10}$$

Here the prefactor is chosen so that integrating over positions and angles yields the total photon flux over the pulse duration T. Eq. (10) is related to the Fourier transformation of the transverse correlation function, and the quantity $T\, B(\boldsymbol{x}, \boldsymbol{\phi})$ can be roughly interpreted as the total number of photons per unit phase-space area in the spectral bandwidth $d\omega$. Due to the wave nature of light, B can take on negative values, so that $B(\boldsymbol{x}, \boldsymbol{\phi}; z)$ is not a true photon number density. For a given electron beam distribution function $f(\boldsymbol{x}, \boldsymbol{x}')$, the total brightness satisfies the convolution theorem [2]

$$\begin{aligned} B(\boldsymbol{x}, \boldsymbol{\phi}, z) = & N_e \int d\boldsymbol{x}_j d\boldsymbol{x}'_j \\ & \times B_j(\boldsymbol{x} - \boldsymbol{x}_j, \boldsymbol{\phi} - \boldsymbol{x}'_j, z) f(\boldsymbol{x}_j, \boldsymbol{x}'_j, z), \end{aligned} \tag{11}$$

where the index j is meant to refer to any single electron, since we have assumed that the particle probability distribution functions are identical and independent. Equation (10) defines the peak brightness for a single pulse. Given the pulse repetition rate f, the average brightness can be calculated via $B_{avg} = BTf$.

UNDULATOR RADIATION

Brightness

The central cone of undulator radiation emitted by a single electron has the rms divergence and source size as [2]

$$\sigma_{r'} = \sqrt{\frac{\lambda}{2L_u}}\,, \quad \sigma_r = \frac{\sqrt{2\lambda L_u}}{4\pi}\,, \tag{12}$$

where the angular divergence and the effective source size is chosen to satisfy $\sigma_r\sigma_{r'} = \lambda/4\pi$, and $\lambda = 2\pi c/\omega$ is the on-axis undulator resonant wavelength. Strictly speaking, the undulator central cone distribution is non-Gaussian, and more detailed approaches have been developed to rigorously describe undulator brightness and transverse coherence [3, 4, 5]. For simplicity, we adopt the Gaussian approximation to write the undulator brightness at $z = 0$ as

$$B_1(\boldsymbol{x}, \boldsymbol{\phi}) \approx \frac{F_1(\omega)}{(\lambda/2)^2} \exp\left(-\frac{\boldsymbol{x}^2}{2\sigma_r^2} - \frac{\boldsymbol{\phi}^2}{2\sigma_{r'}^2}\right), \tag{13}$$

where $F_1(\omega)$ is the photon flux of a single electron within a spectral bandwidth (typically taken to be 0.1%). If we also assume that the electron beam distribution is a Gaussian:

$$f(\boldsymbol{x}_j,\boldsymbol{x}'_j) = \frac{1}{(2\pi)^2\sigma_x\sigma_y\sigma_{x'}\sigma_{y'}} \times \exp\left(-\frac{x_j^2}{2\sigma_x^2} - \frac{y_j^2}{2\sigma_y^2} - \frac{x_j'^2}{2\sigma_{x'_j}^2} - \frac{y'^2}{2\sigma_{y'}^2}\right), \tag{14}$$

than the convolution theorem (11) yields

$$B(\boldsymbol{x},\boldsymbol{\phi}) = \frac{N_e F_1(\omega)}{(2\pi)^2\Sigma_x\Sigma_y\Sigma_{x'}\Sigma_{y'}} \times \exp\left(-\frac{x^2}{2\Sigma_x^2} - \frac{y^2}{2\Sigma_y^2} - \frac{\phi_x^2}{2\Sigma_{x'}^2} - \frac{\phi_y^2}{2\Sigma_{y'}^2}\right), \tag{15}$$

where the convolved rms widths are defined as

$$\Sigma_{x,y}^2 \equiv \sigma_{x,y}^2 + \sigma_r^2\,, \quad \Sigma_{x',y'}^2 \equiv \sigma_{x',y'}^2 + \sigma_{r'}^2\,. \tag{16}$$

The invariant source strength is given by the brightness at the phase space origin, $B(\mathbf{0}, \mathbf{0})$. Two simple limits of the invariant source brightness can be readily obtained from (15). In the emittance dominated regime when $\sigma_{x,y} \gg \sigma_r$ and $\sigma_{x',y'} \gg \sigma_{r'}$, we have

$$B(\mathbf{0}, \mathbf{0}) = \frac{N_e F_1(\omega)}{(2\pi)^2\sigma_x\sigma_{x'}\sigma_y\sigma_{y'}} = \frac{F(\omega)}{(2\pi)^2\varepsilon_x\varepsilon_y}, \tag{17}$$

In the radiation dominated regime when $\sigma_r \gg \sigma_{x,y}$ and $\sigma_{r'} \gg \sigma_{x',y'}$, we have

$$B(\mathbf{0}, \mathbf{0}) = \frac{F(\omega)}{(2\pi)^2\sigma_r^2\sigma_{r'}^2} = \frac{F(\omega)}{(\lambda/2)^2}. \tag{18}$$

We see that $B(\mathbf{0}, \mathbf{0})$ reaches maximum for Eq. (18) when the beam emittance is much less than $\lambda/4\pi$ (the so-called diffraction limit). To maximize the brightness Eq. (15) when the beam emittances are not negligible, it is importance to match the electron and the radiation phase space by taking beta function in the undulator to $\beta_{x,y} \approx L_u/(2\pi)$.

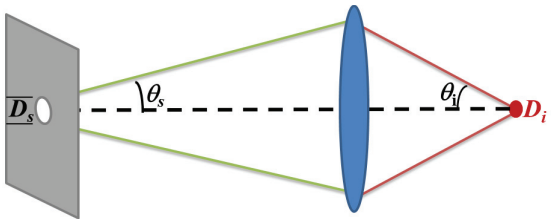

Figure 2: A pinhole is used to spatially filter a partially coherent source to form a small spot after an imaging system. Spatial filter helps until reaching the diffraction limit.

Transverse coherence

A beam with large transverse emittances emits radiation comprises of many transverse modes and hence has a small coherence fraction. Given brightness function Eq. (15), one can take the inverse Fourier transform according to Eq. (10) to obtain the transverse correlation function $\gamma(\boldsymbol{x}_1, \boldsymbol{x}_2)$. Then the degree of transverse coherence or the coherent fraction can be computed from Eq. (8) as:

$$\zeta = \frac{(\lambda/4\pi)^2}{\Sigma_x\Sigma_{x'}\Sigma_y\Sigma_{y'}}\,. \tag{19}$$

For experiments carried out in current third-generation light sources that require full transverse coherence or small focused spots, pinholes or slits are used to filter out extra transverse modes of the photon beam. Consider a perfect focusing system as shown in Fig. 2. The source size is determined by pinhole diameter D_s with the source divergence θ_s (in either x or y plane). A perfect lens conserves the radiation phase space so that the image size $D_i = D_s\theta_s/\theta_i$, where θ_i is the numerical aperture of the lens. As we reduce the pinhole diameter D_s, the image size decreases at the expense of photon flux until the spot reaches the diffraction limit given by $D_i\theta_i \sim \lambda/2$. At that point further reduction in the size of the pinhole only decreases the photon flux without affecting the focused spot size. If the source itself is diffraction limited, i.e., $D_s\theta_s \sim \lambda/2$ in the absence of the aperture, all photon flux can be used in such an experiment. With Gaussian approximation, electron beam emittances must be smaller than $\lambda/(4\pi)$ to produce nearly diffraction limit radiation.

FREE ELECTRON LASERS

Transverse Coherence and Brightness

For a sufficiently bright electron beam and a long undulator, the undulator radiation in the forward direction can be amplified by FEL interaction, leading to an exponential growth of the radiation power along the undulator distance as shown in Fig. 3. Such a self-amplified spontaneous emission (SASE) FEL does not require an optical cavity or a coherent seed and can operate in the x-ray regime. The power gain length in the 1D theory is

$$L_G = \frac{\lambda_u}{4\pi\sqrt{3}\rho}\,, \tag{20}$$

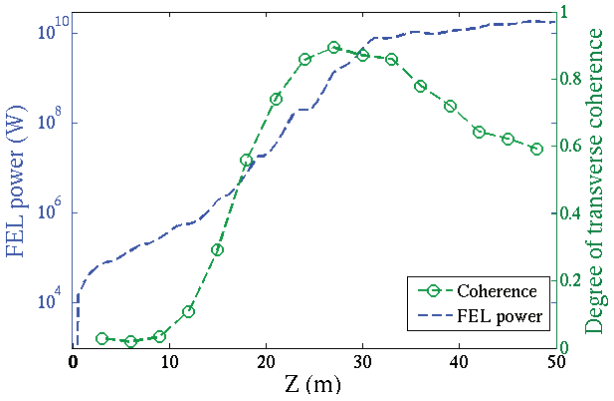

Figure 3: FEL power (blue) and degree of transverse coherence (green) along the LCLS undulator distance for 800 eV photon energy based on start-to-end simulations [6].

where ρ is the FEL Pierce parameter [7]. An x-ray FEL typically requires about 18 gain lengths to reach power saturation. Due to the gain guiding, a single Gaussian-like transverse mode dominates and the transverse coherence approaches 100% near saturation. In the x-ray regime, the transverse mode size and angular divergence are [8]

$$\sigma_r \approx \sqrt{\sigma_x \sigma_D}\,, \quad \sigma_{r'} \approx \frac{\lambda/(4\pi)}{\sigma_r}\,, \tag{21}$$

where $\sigma_D = \sqrt{L_G \lambda/(4\pi)}$. The rms bandwidth is comparable to ρ, which is typically 0.1%. The coherence time τ_c is ~ 1 fs in view of Eq. (6). Since the electron bunch length and hence the x-ray pulse duration are on the order of 100 fs, the number of temporal modes is about 100.

The SASE transverse field profiles produced by simulations can be used in Eq. (8) to analyze the degree of transverse coherence. Figure 3 shows such an example in the LCLS soft x-ray regime [6]. The maximum degree of transverse coherence is reached near saturation (90%) but drops to 60% after saturation. Thus, Eq. (18) can be applied to FEL photon flux at saturation to estimate its brightness. The degree of vertical coherence is measured for the LCLS beam at the soft x-ray photon energy 780 eV ($\lambda \approx 1.6$ nm) [9] using the Young's double slit setup. The amplitude of the transverse correlation function is measured as shown in Fig. 4 for a focused beam size (FWHM) of 17μm after 50 m undulator length. The degree of vertical coherence is about 75% (Fig. 4) while the total degree of transverse coherence (both x and y) is estimated to be 56%, in agreement with simulations.

A comparison of coherence and brightness of undulator radiation and FELs in the x-ray regime are listed in Table 1. Taken together, the improvement of the peak brightness of x-ray FELs over third-generation synchrotron sources can be more than nine orders of magnitude (see Fig. 5). The average brightness of x-ray FELs depends on the linac repetition rate and can still have a large improvement factor.

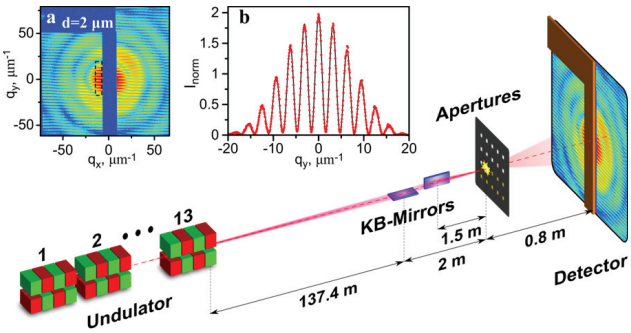

Figure 4: Young's double slit experiment to determine the LCLS transverse coherence at the photon energy 780 eV (courtesy I. Vartanyants) (details see Ref. [9]).

Table 1: Typical Coherence and Brightness of Present Undulator Radiation (UR) and FEL Sources near 1 Å Wavelength

Characteristics	**UR**	**FEL**
radiation	incoherent	coherent
transverse coherence	partial	close to full
transv. coh. fraction	~ 0.01	0.5-1
temporal coherence	partial	partial
# of temporal modes	$\sim 10^6$	$\sim 100^*$
peak brightness	$\sim 10^{24}$	$\sim 10^{33*}$
average brightness	$\sim 10^{20}$	$\sim 10^{22\dagger}$

Brightness unit is photons/s/mrad^2/m^2/0.1%BW.
*Seeding can significantly reduce # of temporal modes and increase the peak brightness.
†Assume a linac repetition rate of 120 Hz.

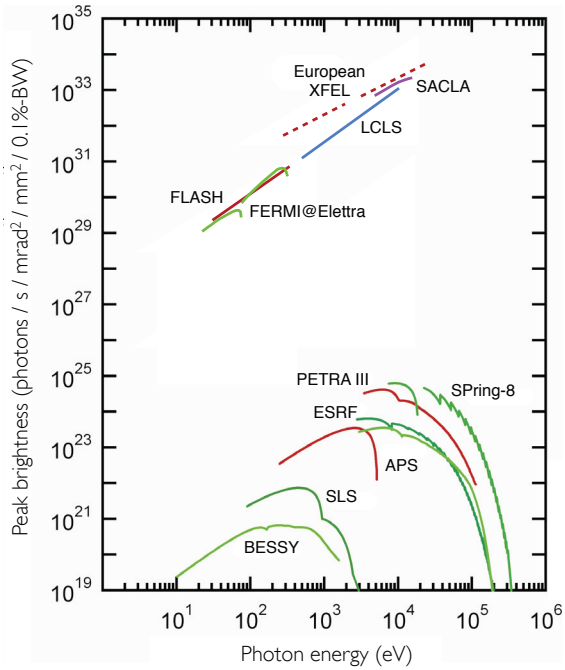

Figure 5: Peak spectral brightness (brilliance) of third and fourth generation accelerator-based light sources.

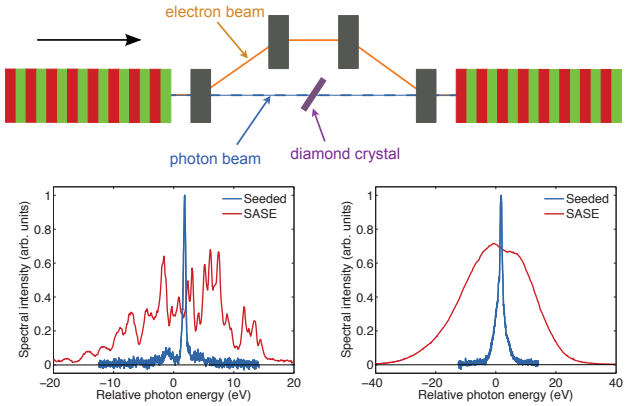

Figure 6: LCLS hard x-ray self-seeding setup (top). Comparison of SASE and seeded spectra at 8.4 keV (bottom), single shots (left) and average spectra (right).

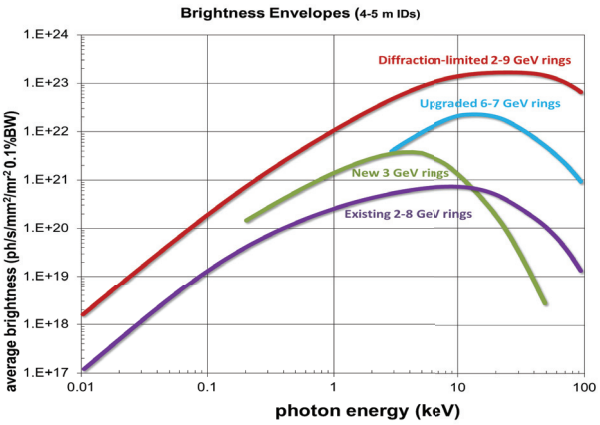

Figure 7: Average brightness envelope of existing, new, upgraded and diffraction-limited storage rings.

Seeding to Enhance Temporal Coherence

Although the poor temporal coherence of a SASE pulse can be improved by a final narrow-bandwidth monochromator, the radiation energy will at least be reduced by the ratio of the SASE bandwidth to the monochromator bandwidth. In order to provide fully coherent x-ray FEL pulses, the intrinsic noise of the SASE radiation must be overcome with some form of seeding. Self-seeding [10] is an effective way to improve SASE temporal coherence. It consists of two undulators and an x-ray monochromator located between them (see Fig. 6). The first undulator operates in the exponential gain regime of a SASE FEL. After the exit of the first undulator, the electron beam is guided through a dispersive bypass that smears out the microbunching induced in the first undulator. The SASE output enters the monochromator, which selects a narrow band of radiation. At the entrance of the second undulator the monochromatic x-ray beam is combined with the electron beam and is amplified to and beyond the saturation power. A simple self-seeding scheme in the hard x-ray regime is recently demonstrated on the LCLS [11] with the bandwidth reduction of a factor 40-50 (Fig. 6).

FUTURE OUTLOOK

Despite spectacular successes in synchrotron radiation and FELs, light source development shows no sign of slowing down. For synchrotron radiation sources, there are very active R&D in diffraction-limited storage rings and energy recovery linacs. The diffraction limited sources require that the beam transverse emittances are less than $\lambda/(4\pi) \sim 8$ pm for $\lambda = 1$Å. As shown in Fig. 7, the average brightness of such sources will be another 2 orders of magnitude brighter than the existing third-generation storage rings in the hard x-ray photon range. High-gain FEL and x-ray oscillator options may be considered to further expand their scientific reaches.

For linac-based FEL sources, there are still tremendous potentials to enhance both the peak and average brightness, and to control the radiation characteristics including polarization, pulse durations and spectral profiles. The peak brightness can be improved by seeding and by tapered undulator in the saturation regime to at least another 2 orders of magnitude. The average brightness of FELs can be improved several orders of magnitude by high-repetition rate linacs from kHz up to MHz.

Last but not the least, plasma wakefield and other advanced accelerator techniques hold promises to generate extremely bright and ultrashort electron beams. Together with advances in novel undulator technology, soft x-ray or even hard x-ray FELs may be produce with footprints much smaller than the large FEL facilities. Taking advantage of the electron's betatron motion in the plasma channel, the beam-radiation interaction in a plasma accelerator may lead to new ways of coherent radiation generation.

ACKNOWLEDGMENTS

I thank D. Attwood, C. Behrens, Y. Cai, J. Corbett, Y. Feng, B. Hettel, K.-J. Kim, R. Lindberg, T. Rabedeau, G. Stupakov for useful discussions and inputs.

REFERENCES

[1] J. Goodman, *Statistical Optics* (Wiley, 2000).

[2] K.-J. Kim, AIP Conference Proceedings **184**, 565 (1989).

[3] A. Hofmann, *The Physics of Synchrotron Radiation* (Cambridge, 2004).

[4] G. Geloni *et al.*, Nucl. Instrum. Methods A **588**, 463 (2008).

[5] I. Bazarov, PRSTAB **15** 050703 (2012).

[6] Y. Ding, Z. Huang, S. Ocko, MOPC16, FEL2010.

[7] R. Bonifacio, C. Pellegrini, and L. M. Narducci, Opt. Commun. **50**, 373 (1984).

[8] Z. Huang and K.-J. Kim, PRSTAB **10**, 034801 (2007).

[9] I. Vartanyants *et al.* PRL **107** 144801 (2011).

[10] J. Feldhaus *et al.*, Opt. Commun. 140, 341 (1997).

[11] J. Amann *et al.*, Nature Photonics **6** 694 (2012).